

# Horizontal Pyramid Matching for Person Re-identification

Yang Fu<sup>1\*</sup>, Yunchao Wei<sup>1\*</sup>, Yuqian Zhou<sup>1</sup>, Honghui Shi<sup>2,1</sup>  
 Gao Huang<sup>3</sup>, Xinchao Wang<sup>4</sup>, Zhiqiang Yao<sup>5</sup>, Thomas Huang<sup>1</sup>

<sup>1</sup>IFP, Beckman, UIUC, <sup>2</sup>IBM Research, <sup>3</sup>Cornell University, <sup>4</sup>Stevens Institute of Technology, <sup>5</sup>CloudWalk Technology  
 {yangfu2, yunchao, yuqian2, t-huang1}@illinois.edu, honghui.shi@ibm.com  
 gh349@cornell.edu, xinchao.wang@stevens.edu, yaozhiqiang@cloudwalk.cn

## Abstract

Despite the remarkable recent progress, person re-identification (Re-ID) approaches are still suffering from the failure cases where the discriminative body parts are missing. To mitigate such cases, we propose a simple yet effective Horizontal Pyramid Matching (HPM) approach to fully exploit various partial information of a given person, so that correct person candidates can be still identified even if some key parts are missing. Within the HPM, we make the following contributions to produce a more robust feature representation for the Re-ID task: 1) we learn to classify using partial feature representations at different horizontal pyramid scales, which successfully enhance the discriminative capabilities of various person parts; 2) we exploit average and max pooling strategies to account for person-specific discriminative information in a global-local manner; 3) we introduce a novel horizontal erasing operation during training to further resist the problem of missing parts and boost the robustness of feature representations. Extensive experiments are conducted on three popular benchmarks including Market-1501, DukeMTMC-reID and CUHK03. We achieve mAP scores of 83.1%, 74.5% and 59.7% on these benchmarks, which are the new state-of-the-arts.

## 1. Introduction

Person re-identification (Re-ID) aims at re-identifying a query person from a collection of images, for example, taken by multiple cameras across time. It is challenging because of large variations of human attributes like poses, gaits, clothes, as well as the environmental settings like illumination, complex background, and occlusions. To address the complexities of the visual cues, deeply-learned features have been applied and have proven to be more effective than hand-crafted ones [39, 32, 39, 33, 27].

\* authors contribute equally

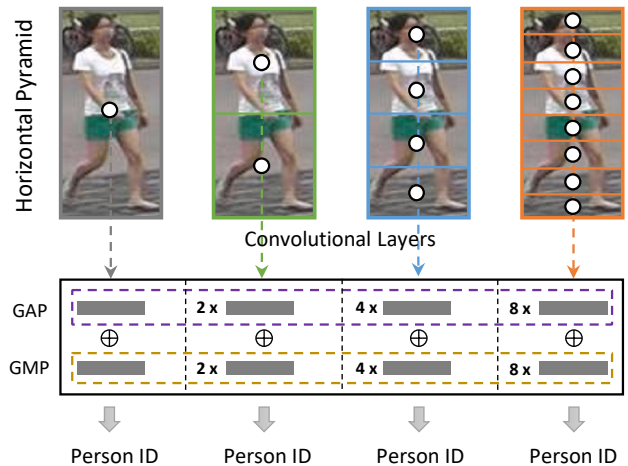


Figure 1. Illustration of the proposed Horizontal Pyramid Matching. We split a person into different horizontal parts of multiple scales. The feature representations produced by Global Average Pooling (GAP) and Global Max Pooling (GMP) of each part are then leveraged to learn to the person Re-ID independently.

Many recent approaches have been focusing on learning partial discriminative feature representations. These methods usually take advantage of global features like body size and local ones like cloths logo, to enhance the robustness of the Re-ID methods. They can be categorized into three types based on the local-region generation scheme. In the first type, prior knowledge like poses or body landmarks are estimated and extracted to localize the discriminative regions [25, 40, 30]. However, the performance of Re-ID in this case highly relies on the robustness of the pose or landmark estimation models. Unexpected errors like erroneous estimation of poses may greatly influence the identification result. The second type, attention-based approaches [22, 21, 38, 19], focus on extracting the salient regions of interest (ROI) adaptively by localizing the high activations in the deep feature maps. The selected regions however lack semantic interpretation. The third type of methods crop

deep feature maps into pre-defined patches or stripes by assuming the images are perfectly aligned [27, 16], and are thus prone to errors introduced by outliers.

Person Re-ID also benefits from proper data augmentation methods. Recent work takes advantage of Generative Adversarial Networks (GANs) [10, 45] to synthesize images of different human poses [14], camera styles [48], and person across different domains [29]. However, such methods suffer from longer training time, convergence issues and low-quality generation. Integrating the generative and discriminative models requires multi-stage training and testing, which can not be achieved in an end-to-end fashion.

In this paper, we focus on learning partial discriminative features to boost the performance of person Re-ID. We propose a simple yet effective Horizontal Pyramid Matching (HPM) approach, in aim to fully exploit global and partial information of a person for the Re-ID task. Specifically, we make three contributions as follows.

- We slice the deep feature maps horizontally using pyramid scales for pooling, which we name as Horizontal Pyramid Pooling (HPP), and learn to classify each partial feature independently. Intuitively, using multiple scales of strips will incorporate a slack distance to mitigate the outliers issue caused by misalignment. Also, learning multi-scale information independently will enhance the discriminative information learned in all the scale-specific person parts.
- We combine the average and max pooling features in each partition. Average pooling accounts for global information but is sensitive to unrelated background patterns, while max pooling extracts the most salient local features but ignores discriminative information. Integrating them both thus balance the effectiveness of these two strategies in a global-local manner.
- We apply random horizontal erasing operation to augment the training data on the fly to simulate occlusions or key parts missing cases in the original images. This is achieved by randomly zeroing-out multiple rows of deeply learned features before the HPP layer during training.

We show an example of the proposed HPM in Figure 1, where we horizontally slice the feature maps at multiple scales. The feature representations generated by both global average pooling and global max pooling of each part are then employed to conduct Re-ID independently. By learning the HPM in such a manner, we expect the partial discriminative capability to be enhanced. Figure 2 shows the heatmaps of the last convolutional feature maps learned by w/ HPM and w/o HPM schemes. It is observed that more discriminative parts can be identified by our HPM, which leads to better person Re-ID results.

Extensive experiments and ablation study conducted on Market-1501, DukeMTMC-reID and CUHK03 have demonstrated the effectiveness of each design. In particular, we achieve the mAP scores of 83.1%, 74.5% and 59.7% on the three benchmarks, which outperform the state-of-the-arts more than 1.5%, 5.3% and 2.2%, respectively.

## 2. Related Work

In this section, we review several closely related work including deep learning methods for Person Re-ID, part-based models, spatial pyramid pooling and data augmentation.

### 2.1. Deep learning for Person Re-ID

Deep learning based method has dominated in Re-ID community [42]. Yi *et al.* [35] first employed deep neural network to determine if a pair of input images belong to the same ID. In general, two types of models are used for person retrieval: verification and identification model.

For the verification model, a pair or a triplet of images are fed into a siamese neural network [3, 1, 13, 8, 5, 17]. In [13], Hermans *et al.* proposed a variant of triplet loss to perform end-to-end deep metric learning, which can outperforms many other published methods by a large margin. However, generally, this kind of model may have a compromised efficiency on large gallery. This is because it does not make full use of re-ID annotations. Giving the siamese model information about whether an image pair is similar or not is a weak label in Re-ID.

For the identification model [32, 39, 33, 27], it always yields superior accuracy compared with verification model. Xiao *et al.* [32] propose a novel dropout strategy to train a classification model with multiple datasets jointly. In [43], the verification and classification losses are combined together to learn a discriminative embedding and a similarity measurement at the same time. In [27], a Part-based Convolutional network is proposed to learn discriminative part-informed features.

### 2.2. Part-based Model

Recently, many works generate deep representation from local parts for fine-grained discriminative features of pedestrian. This kind of part-based model can be divided into three categories. First one is based on some prior knowledge like pose estimation and landmark detection[40, 25, 30]. These methods share a same drawback that is the gap lying between datasets for pose estimation and person retrieval. Second, several other works abandon the semantic cues for partition[34, 22, 38, 19]. For example, Yao *et al.* [34] employed the Part Loss Networks which enforces the deep network to learn representations for different parts and gain the discriminative power on unseen persons. Third, the partition is cropped into pre-defined patches[27, 16]. Sun *et al.* [27] proposed Part-based Convolutional Baseline

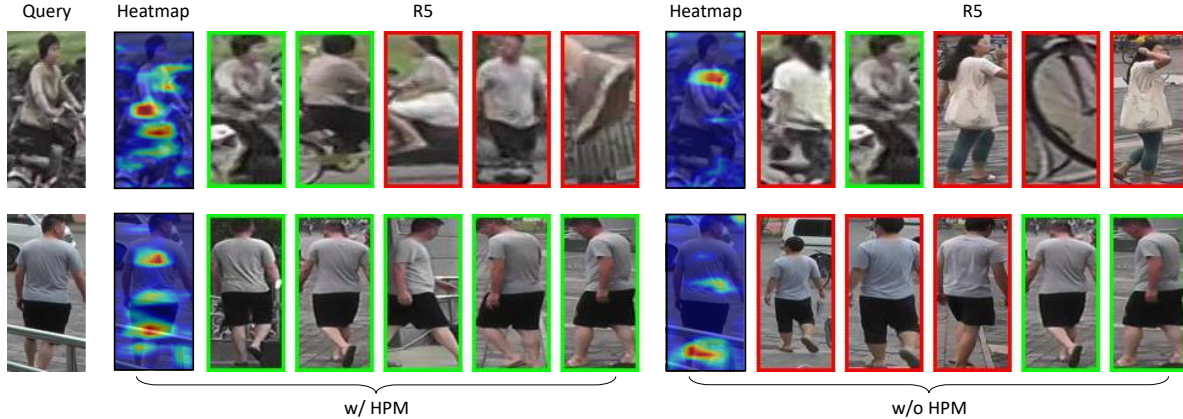


Figure 2. Comparisons of results w/ HPM and w/o HPM in Person Re-ID.

(PCB) to learn discriminative partition features. However, the PCB may suffer some outliers, which make the inconsistency in each partition, thus they proposed Refined Part Pooling (RPP) to enhance within-part consistency.

### 2.3. Spatial Pyramid Pooling

Since convolutional neural networks with the fully connected layer always require the fixed input size. In order to remove this constrain, He *et al.* [11] proposed the Spatial Pyramid Pooling network, which is able to generate a fixed length output regardless of the input size and maintain spatial information by pooling in local spatial bins. Multi-level spatial pooling has also shown to be robust to object deformations. It can improve the performance of classification and object detection tasks. Similarly pyramid pooling module is also used in [37], the pyramid level pooling separates the feature map into different sub-regions and forms pooled representation for different locations.

### 2.4. Region Erasing

Region erasing is firstly presented by Wei *et al.* [31], which proposed an Adversarial Erasing (AE) for densely localizing object-related pixels in a weakly-supervised manner. However, Wei *et al.* [31] adopted a step-wise training strategy to mine new object regions by progressively erasing the discovered ones, which is time-consuming. Singh *et al.* [24] proposed a Hide-and-Seek approach similar to AE, which splits the input image into multiple squared grids and randomly erases some of them. In addition, Zhong *et al.* [47] also adopted a similar erasing approach as [24], which randomly selects a rectangle region in an input image and erases its pixels with random values. All these works has well demonstrated the effectiveness of the region erasing strategy in enhancing the discriminative abilities of object parts. Motivated by the previous works, we propose a simple horizontal random erasing (HRE) method in this work, which augments our HPM to achieve better

Re-ID results. Different from [31, 24, 47] that conducts erasing operation on the original input images, we consider each horizontal row as an independent unit and randomly erase several of them through the zero-out operation from the learned feature maps. Our method can be also regarded as a data augmentation trick for person Re-ID task and can be easily embedded in any other frameworks for further performance improvement.

## 3. Proposed Method

This section describes the structure of Horizontal Pyramid Matching (HPM) framework as shown in Fig 3. The input image is fed into the a backbone network to extract the feature maps. After that, we use horizontal spatial pyramid pooling module to obtain spatial information in each local and global spatial bin. During this step, in order to improve the robustness of the model, we randomly erase several spatial bins from the feature maps horizontally. For each horizontal spatial bin, we use both global average pooling operation and max pooling operation. Then, convolutional layers are used to reduce the dimensions of the column feature maps from 2048 to 256 and each column feature is input into a non-share fully connected layer and followed by a softmax function to predict the ID of each input image. During testing, all these features are concatenated together to obtain the final features.

### 3.1. Horizontal Pyramid Matching

**Backbone Network** The HPM can take various network architecture like VGG [23], Resnet [12] and Google Inception [28] as the backbone. Our paper choose the Resnet50 as backbone network. There are some modifications on the original Resnet50. First, the average pooling layer and the fully connected layer are removed. Also, the stride of the conv4\_1 is set to 1. As a result, the size extracted feature maps should be  $\frac{1}{16}$  of the input image size.

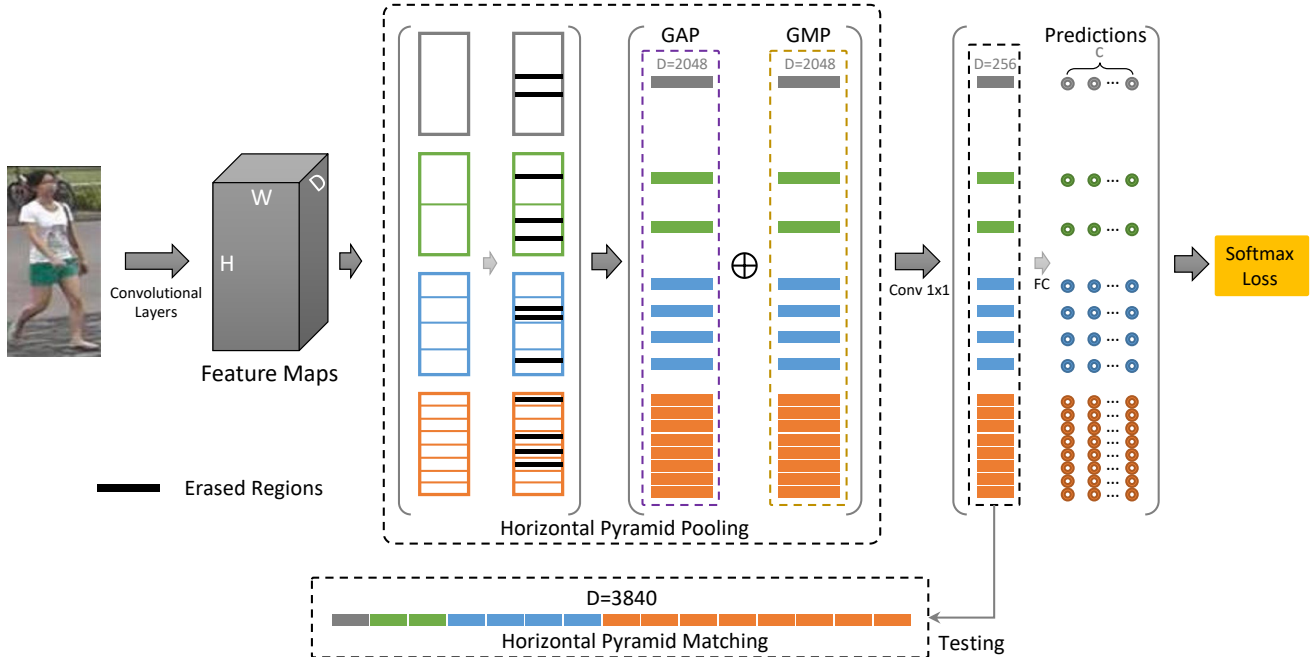


Figure 3. Overview of the proposed Horizontal Pyramid Matching (HPM) approach. The input image firstly goes through a convolutional neural network to extract its feature maps. Then, the horizontal pyramid pooling is leveraged to producing feature representation of each part using both global average pooling and global max pooling. At this stage, we adopt a simple yet effective horizontal random erasing operation to augment the HPM for learning more robust representations. Finally, prediction of each part is fed into the classifier to conduct partial-level person re-id. During the testing stage, we concatenate features of parts at different pyramid scales to form the final feature representation of each image.

**Horizontal Pyramid Pooling module** The convolutional networks only accept arbitrary input sizes and the output of the fully connected layer is a fixed length vector, which is contrast to the face that the pedestrian sizes and discriminative parts vary from image to image. In [11], He *et al.* proposed Spatial Pyramid Pooling (SPP) to deal with multi-size inputs. SPP has 4 scales and each scale splits the feature maps into specific number of spatial bins and do max pooling of each bin. With the same intuition, we propose the horizontal pyramid pooling module, which splits and pools the feature maps vertically. We do this pyramid pooling horizontally because the distribution of distinguish partitions of a pedestrian is from head to foot. By doing this, we can obtain a fixed length vector for different pedestrian size and different partitions of pedestrian, which is needed by fully connected layers and softmax function. In addition, these different scales pyramid pooling have the ability to capture the discriminative partition of pedestrian from coarse to fine, from global to local.

Specifically, our horizontal Pyramid Pooling module has 4 scales and in each scale the feature maps extracted by backbone network  $F$  is splitted into several spatial bins horizontally and equally. Denote each spatial bin as  $F_{i,j}$ .  $i, j$  stand for the index of scale and the index of bins in each

scale, so  $F_{3,4}$  means the fourth bin in third pooling scale. Then, we pool each spatial bin  $F_{i,j}$  by global average and max pooling to generate column feature vector,  $G_{i,j}$ .

$$G_{i,j} = \text{avgpool}(F_{i,j}) + \text{maxpool}(F_{i,j})$$

After that each  $G_{i,j}$  is input into a convolutional layer to reduce the dimensions from 2048 to 256,  $H_{i,j}$ . These  $H_{i,j}$  with the same  $i$  can be considered as a description of the pedestrian. This kind of description covers more detailed features with the increasing of scales index  $i$ .

**Loss Function** In this paper, we use the classification model to deal with the Person Re-ID, so the goal is to predict the ID of each pedestrian. We use a branch of fully connected layer as classifier, each feature column vector  $H_{i,j}$  is fed into a corresponding classifier  $FC_{i,j}$  and following a softmax function to predict its ID. During training, the output of given image  $I$  is a set of predictions  $\hat{y}_{i,j}$ . Each  $\hat{y}_{i,j}$  can be formulated as

$$\hat{y}_{i,j} = \underset{c \in P}{\operatorname{argmax}} \frac{\exp((W_{i,j}^c)^T H_{i,j}(I))}{\sum_{p=1}^P \exp((W_{i,j}^p)^T H_{i,j}(I))}$$

where the  $P$  is the total number of person ID,  $W_{i,j}$  is the learnt weights of  $FC_{i,j}$ ,  $y$  is the ground truth ID of input

image  $I$ . The loss function is sum of Cross Entropy loss of each output  $\hat{y}_{i,j}$ .

$$Loss = \sum_{n=1}^N \sum_{i,j} CE(\hat{y}_{i,j}^n, y^n)$$

where  $N$  is the size of mini-batch,  $CE$  is the Cross Entropy loss.

### 3.2. Horizontal Random Erasing

In the HPM, we introduce a horizontal erasing operation which can boost the robustness and performance. Zhong *et al.* [47] proposed random erasing as a kind of data augmentation. During training, random erasing randomly selects a rectangle region in an image and erases its pixels with random value. In order to reduce the risk of over-fitting and make our model more robust, we use the same strategy on the feature map level. Specifically, for each batch, instead of selecting a rectangle region, we split feature map  $F$  obtained by the backbone network row by row with a probability of  $p$ , getting 24 column vectors. Then, we randomly choose  $n$  of them and erase those  $n$  vectors with zeros.  $n$  is also generated randomly for each batch. The detailed procedure is show in Alg 1.

---

**Algorithm 1:** Algorithm of Horizontal Random Erasing

---

**Input** : Feature map  $F$ ;  
Size of Feature map,  $h, w$ ;  
Erasing probability  $p_e$ ;

**Output:** Erased Feature map  $F_e$

**Initialization:**  $p = \text{Rand}(0, 1)$

**if**  $p_e \geq p$  **then**  
|  $F_e \leftarrow F$ ;  
| **return**  $F_e$ ;

**end**

**else**  
| **while** *True* **do**  
| |  $n \leftarrow \text{Rand}(1, h)$ ;  $m \leftarrow \text{Shuffle}([1, 2, \dots, h])$ ;  
| |  $F_e \leftarrow F$ ;  
| | **for**  $i = 1 : n$  **do**  
| | |  $F_e(m(i), :) \leftarrow 0$ ;  
| | **end**  
| | **return**  $F_e$ ;  
| **end**  
**end**

---

### 3.3. Testing

During testing, given a query image as  $I_q$ , the goal is to return all images with the same identification from a gallery set  $G$ , denote  $G = I_g, g \in [1, m]$ . The  $I_q$  is first resized to

384x128, then input it into HPM framework to generate several column feature vectors *e.g.*  $[H_{1,1}, H_{2,1}, H_{2,2}, \dots, H_{4,4}]$ , and these vectors are concatenated together as the representation of  $R_q$ . And every image in gallery goes through the same process of query image, generating a list of  $R_g$ . Then, the representation of query image  $R_q$  is compared with every  $R_g$  to compute Rank 1/5/10 and mean average precision.

### 3.4. Variant of HPM

HPM may have some variants different from the basic framework describe above, *e.g.* different pyramid scales and pooling strategies.

**Number of pyramid scales** The HPM can have several different number of scales. Instead of the 4 scales, it can be any number up to the  $\log_2(h)$ , where  $h$  is the height of feature map. The HPM structure with different pyramid scales is shown in Table 1. The model will focus on more detailed and fine partition of the pedestrian with the increasing of pyramid scales. Since our loss function is a linear combination of each pyramid scales, if there are too many pyramid scales, the global information of the pedestrian may be underestimated. On the other hand, if too few pyramid scales, the features of local discriminative partition may be more difficult to extract. Thus, choosing a proper pyramid scales that can balance the global and local features is vital for the performance of HPM.

# PS	# Spatial Bins	Size of Spatial Bins
1	1	24x8
2	1, 2	24x8, 12 x 8
3	1, 2, 4	24 x 8, 12x8, 6x8
4	1, 2, 4, 8	24 x 8, 12x8, 6x8, 3x8

Table 1. HPM Structure with different pyramid scales, PS means the pyramid scale

**Pooling strategies** The HPM uses both average pooling and max pooling. The global average pooling is a traditional operation in many classification framework, because it enforces a corresponding relation between feature maps and categories. However, the global average pooling can lose some very discriminative information by the average operation. For example, if one partition of the pedestrian is very discriminative but surrounded by background, in this case, the global average pooling will obtain the average of the discriminative part and the background, which may lead to a low response and miss it. To deal with this problem, we use both average pooling and max pooling, which can maintain the global relation with the identification and preserve the discriminative part.

## 4. Experiments

In this section, we evaluate the proposed method on three most widely used datasets: Market1501 [41], DukeMTMC-

ReID [45] and CUHK03 [17].

### 4.1. Dataset and Evaluation Protocol

**Market1501** contains 32,668 images of 1,501 labeled persons of six camera views. There are 19,732 gallery images and 12,936 training images detected by DPM [9], including 751 identities in the training set and 750 identities in the testing set. It also contains 500,000 images as some distractors, which may has a considerable influence on the retrieval accuracy.

**DukeMTMC-ReID** is a subset of the DukeMTMC dataset. It contains 1,812 identities captured by 8 cameras. There are 2,228 query images, 16,522 training images and 17,661 gallery images, with 1,404 identities appear in more than two cameras. Also, similar with the Market1501, the rest 408 IDs are considered as distractor images. DukeMTMC-reID is one of the most challenging reID datasets up to now with so many images from 8 multi-cameras.

**CUHK03** consists of 14,097 cropped images from 1,467 identities. For each identity, images are captured from two cameras and there are about 5 images for each view. There are two ways to obtain the annotations: human labeled and detected by DPM. Our evaluation is based on the detected label image.

**Evaluation Protocol** In our experiment, we use Cumulative Matching Characteristic (CMC) curve and the mean average precision (mAP) to evaluate our approach. CMC represents the accuracy of the pedestrian retrieval, it is accurate when each query only has one ground truth. However, when multiple ground truths exist in the gallery, the goal is to return all right match to user. In this case, CMC may not have enough discriminative ability, but the mAP could reflect the recall. For Market-1501 and DukeMTMC-reID. We use the evaluation packages provided by [41] and [45], respectively. And for CUHK03, we adopt the new training/testing protocol proposed in [46]. Moreover, for simplicity, all results reported in this paper is under the single-query setting and does not use the re-ranking proposed in [46].

### 4.2. Implementation Details

In order to obtain enough information from pedestrian image and proper size of feature map for horizontal pyramid pooling, we resize all the image to 384x128. For the backbone network, we use Resnet50 that initialized with the weights pretrained on ImageNet [7]. We remove the last fully connected layer and average pooling layer and set the stride of last resent conv4\_1 from 2 to 1. The training images are augmented with horizontal flipping and normalization. The batch size is set to 64 and we train model for 60 epoch. The base learning rate is set to 0.1 and decay to 0.01 after 40 epochs. Notice that learning rate for all pretrained Resnet layer is set to 0.1 x base learning rate. The

stochastic gradient descent (SGD) with 0.9 momentum is implemented in each mini-batch to update the parameters. During evaluation, we add the features from original image and horizontal flipped image and use the normalized feature for retrieval evaluation. Our model is implemented on Pytorch platform and train with two NVIDIA TITAN X GPUs. All datasets share the same experiments setting as above.

Model	R1	R5	R10	mAP
BoW+kissme [41]	44.4	63.9	72.2	20.8
WARCA [15]	45.2	68.1	76.0	-
SVDNet [26]	82.3	92.3	95.2	62.1
PAN [44]	82.8	-	-	63.4
PAR [38]	81.0	92.0	94.7	63.4
MultiLoss [18]	83.9	-	-	64.4
TripletLoss [13]	84.9	94.2	-	69.1
MultiScale [6]	88.9	-	-	73.1
MLFN [4]	90.0	-	-	74.3
HA-CNN [19]	91.2	-	-	75.7
AlignedReID [36]	91.0	96.3	-	79.4
Deep-Person [2]	92.3	-	-	79.5
PCB [27]	92.4	97.0	97.9	77.3
PCB + RPP [27]	93.8	97.5	98.5	81.6
HPM(ours)	<b>94.2</b>	97.5	<b>98.5</b>	82.7
HPM(ours) + HRE	93.9	<b>97.8</b>	98.3	<b>83.1</b>

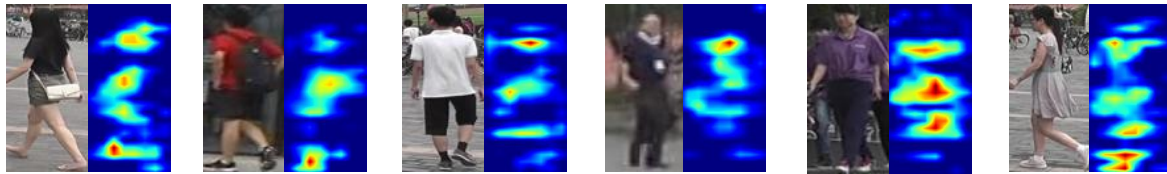
Table 2. Comparison of the proposed method with the art on Market-1501, HPM is implemented with four pyramid scales and combine both average pooling and max pooling, as described in Fig 3. HRE stands for Horizontal Random Erasing

Model	R1	mAP
BoW+kissme [41]	25.1	12.2
LOMO+XQDA [20]	30.8	17.0
PAN [44]	71.6	51.5
SVDNet [26]	76.7	56.8
MultiScale [6]	79.2	60.6
HA-CNN [19]	80.5	63.8
Deep-Person [2]	80.90	64.80
MLFN [4]	81.0	62.8
PCB [27]	81.8	66.1
PCB + RPP [27]	83.3	69.2
HPM(ours)	<b>86.6</b>	74.3
HPM(ours) + HRE	86.3	<b>74.5</b>

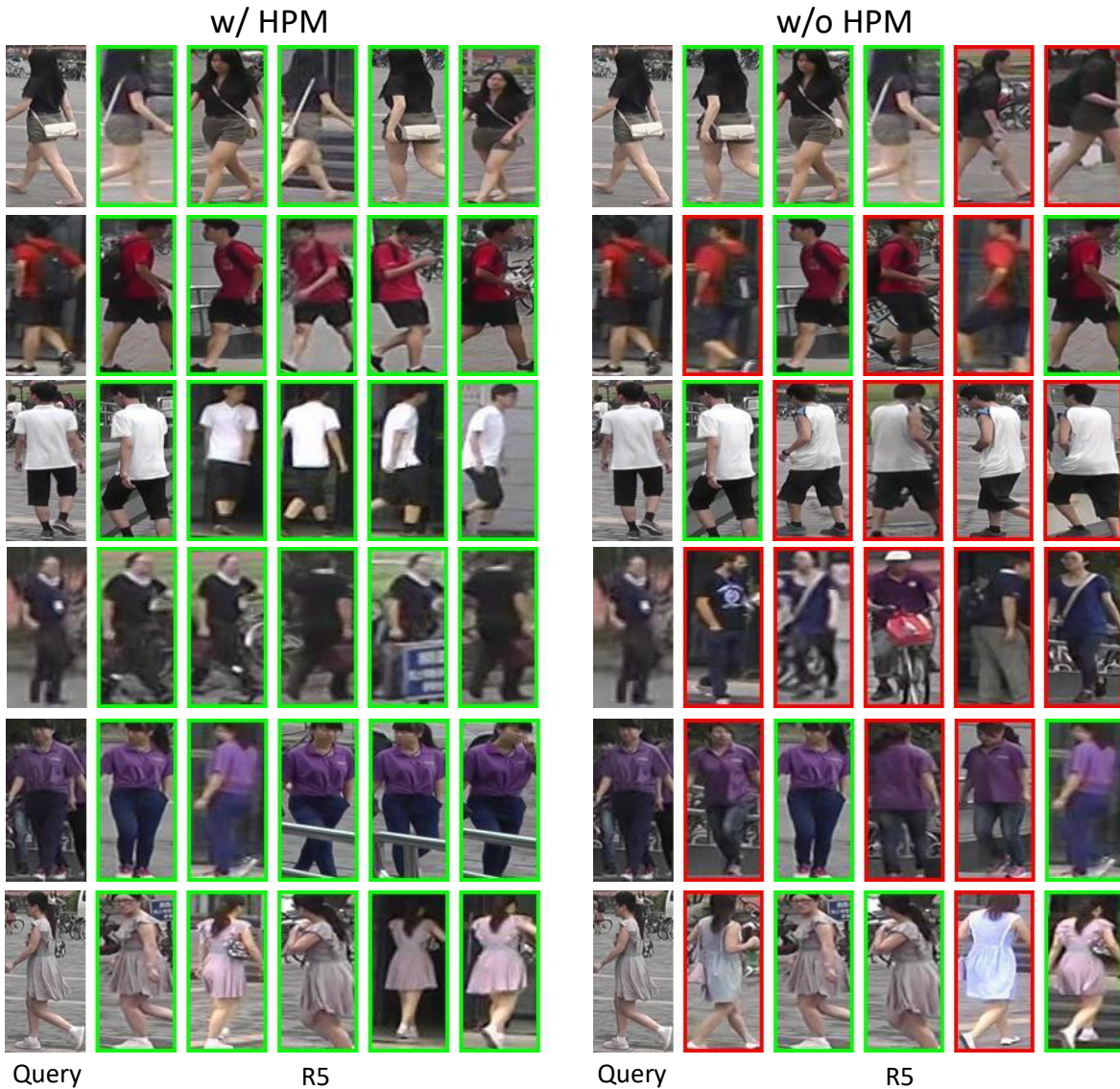
Table 3. Comparison of the proposed method with the art on DukeMTMCreID, HPM is implemented with four pyramid scales and combine both average pooling and max pooling, as described in Fig 3. HRE stands for Horizontal Random Erasing

### 4.3. Comparison with the State-of-the-arts

**Results on Market1501** Comparisons between HPM and state-of-art approaches on Market1501 are shown in Table 2. The results show that our HPM achieves the mAP of



(a)



(b)

Figure 4. Qualitative Results: (a) Queries and the corresponding discriminative heatmaps learned by the proposed HPM. (b) Comparisons of R5 of w/ HPM and w/o HPM schemes.

83.1% and Rank 1 accuracy 94.2%, which both surpass all existing works more than 1.5% and 0.4%, respectively. It should be noted that we do not conduct any post-processing operation (*e.g.* the re-rank algorithm given by [46]), which can further bring a considerably improvement in terms of

mAP. PCB [27] is closest competitor, which also leverages partial-based learning for person Re-ID. However, there are mainly two disadvantages of PCB, *i.e.* 1) it splits the features maps into pre-defined patches (6 in PCB) with the assumption that most persons in the given images are well

Model	R1	mAP
BoW+kissme [41]	6.4	6.4
LOMO+XQDA [20]	12.8	11.5
PAN [44]	36.3	34.0
SVDNet [26]	41.5	37.3
MultiScale [6]	40.7	37.0
HA-CNN [19]	41.7	38.6
MLFN [4]	54.7	49.2
PCB [27]	61.3	54.2
PCB + RPP [27]	63.7	57.5
HPM(ours)	63.1	57.5
HPM(ours) + HRE	<b>63.2</b>	<b>59.7</b>

Table 4. Comparison of the proposed method with the art on CUHK03 Detected set, HPM is implemented with four pyramid scales and combine both average pooling and max pooling, as described in Fig 3. HRE stands for Horizontal Random Erasing

Model	Market1501		
	R1	R5	mAP
No Pyramid Structure	92.0	96.3	76.4
HPM	<b>94.2</b>	<b>97.5</b>	<b>82.7</b>

Table 5. Evaluation of effectiveness of Pyramid Structure, HPM uses four pyramid scales and combine both average pooling and max pooling, Non pyramid structure split the feature into same partitions as the last scale in HPM but without pyramid structure

aligned, which not make scene and resist to some outliers; 2) its state-of-the-art results are benefited from a powerful post-processing approach called RPP, which enable the optimized model cannot be trained in an end-to-end manner. In contrast, our HPM splits the feature maps according to various pyramid scales, which is more robust compared with PCB in addressing the outliers that are not well aligned. In addition, our HPM can be end-to-end learned and we believe that any post-processing operation can make a continued improvements upon the current results. From Table 2, we can observe that our HPM makes a 5.4% improvements compared with PCB in mAP. Even without post-processing, our HPM is still better than PCB+RPP (*i.e.* 83.1% *vs.* 81.6%). Beyond PCB, the best model aims to deal with different size of pedestrian MultiScale [5] yields the mAP of 73.1% and Rank 1 accuracy of 88.9%. Our HPM model outperforms it by 5.3% and 10.0% on Rank 1 and mAP, respectively.

**Results on DukeMTMC-ReID** Person Re-ID results on Duke MTMC-reID are given in Table 3. This dataset is challenging because it has 8 different camera and the person bounding box size varies drastically across different camera views, however, our HPM achieves even better performance on this dataset. Without any post-processing, it still achieves 74.8% on mAP and 86.6% on Rank 1 accuracy, which is better than all other state-of-the-art methods by a large margin, 5.3% and 3.3%. Note that our HPM is the first

model that can achieve above 80% on mAP, which surpass all state-of-the-art methods by more than 5.0%

**Results on CUHK03** Table 4 shows results on CUHK03 when detected person bounding boxes are used for both training and testing. HPM achieves the best result of mAP, 59.7% under this setting. Although the Rank 1 accuracy of HPM is a little lower than PCB+RPP, there’s a clear gap, more than 2%, between HPM and other methods, including the PCB+RPP, on mAP. And We believe that, as a end-to-end and part-based model, the RPP can also boost the performance HPM further.

**Qualitative Result** We visualize some examples in Figure 4. Concretely, Figure 4 (a) shows the queries and the corresponding heatmaps<sup>1</sup> of the last convolutional feature maps. We observe that the discriminative abilities of multiple person parts are enhanced with our HPM. Figure 4 (b) compares the Re-ID results of w/ HPM and w/o HPM schemes. It can be seen that our HPM is very effective in guaranteeing accurate Re-ID results.

#### 4.4. Ablation Study

To verify the effectiveness of each component and setting of HPM, we design several ablation study with different settings on Market-1501, DukeMTMC-ReID and CUHK03, including different number of pyramid scales, w/ and w/o using pyramid structure, different pooling strategies, w/ and w/o horizontal random erasing. Note that all unrelated settings are the same as HPM implementation detailed in Section 4.2

**Number of Pyramid Scales** Table 6 shows the Re-ID results of HPM with different pyramid scales, *i.e.* 1, 2, 4, 8. From these results, we can find that HPM reaches the best performance with four pyramid scales. Intuitively, the number of pyramid  $p$  determines the granularity of the partition feature. When  $p = 1$ , it is equivalent to global pooling. With the increasing the number of  $p$ , Rank 1 accuracy and mAP are significant improved from 88.1% and 71.2% to 93.2% and 79.5%. The reason why the HPM does not drops dramatically at some point as introduced in [27] is that the pyramid structure can combine both global and local features, which may increase the discriminative ability of very small partition. Since the last convolutional feature maps are with 24 horizontal units, we also try more dense pyramid scales, such as 12 and 24. However, more pyramid scales will bring additional computational cost and there is no obvious improvement can be observed. Therefore, we finally adopt 4 pyramid scales in this work.

**Effectiveness of Pyramid Structure** Previous analysis shows that the HPM reaches the best performance with four pyramid scales, which has up to 8 partial bins on the feature map. In order to verify the effectiveness of pyramid struc-

<sup>1</sup>We normalize each feature map of the last convolutional feature maps and sum them together to obtain the heatmap.

Model	Feature Dim	Market1501				DukeMTMC-ReID				CUHK03			
		R1	R5	R10	mAP	R1	R5	R10	mAP	R1	R5	R10	mAP
HPM + #PS 1 + Avg pool	256	88.1	94.6	96.4	71.2	79.3	89.7	91.9	61.0	39.2	61.1	71.6	37.3
HPM + #PS 2 + Avg pool	256x(1+2)	92.0	96.9	97.9	78.3	83.1	91.9	93.4	68.9	53.2	73.2	79.6	48.9
HPM + #PS 3 + Avg pool	256x(1+2+4)	92.3	97.2	97.9	79.3	84.5	92.4	94.1	70.8	58.2	76.7	83.1	52.8
HPM + #PS 4 + Avg pool	256x(1+2+4+8)	93.2	97.3	98.1	79.5	84.8	92.5	94.1	72.1	58.6	76.8	83.8	53.4
HPM + #PS 4 + Max pool	256x(1+2+4+8)	93.6	<b>97.7</b>	98.3	81.6	86.2	<b>93.2</b>	94.8	74.1	62.4	78.9	<b>86.3</b>	57.4
HPM + #PS 4 + Max+Avg pool	256x(1+2+4+8)	<b>94.2</b>	97.5	<b>98.5</b>	<b>82.7</b>	<b>86.6</b>	93.0	<b>95.1</b>	<b>74.3</b>	<b>63.1</b>	<b>79.7</b>	86.1	<b>57.5</b>

Table 6. Performance comparison of the proposed method with different pyramid scales and different pooling strategies as described in Section 3.4. PS mean the pyramid scales of HVM

Model	Market1501			DukeMTMC-ReID			CUHK03		
	R1	R5	mAP	R1	R5	mAP	R1	R5	mAP
HPM	<b>94.2</b>	97.5	82.7	<b>86.6</b>	92.8	74.3	63.1	79.7	57.5
HPM + HRE	93.9	<b>97.8</b>	<b>83.1</b>	86.3	<b>93.0</b>	<b>74.5</b>	<b>63.2</b>	<b>80.9</b>	<b>59.7</b>

Table 7. Evaluation of effectiveness of Horizontal Random Erasing, HPM uses four pyramid scales and combine both average pooling and max pooling. HRE stands for Horizontal Random Erasing

ture, we remove other branches and just preserve the branch with 8 partial bins. From Table 5, we can observe that Rank 1, Rank 5 and mAP drop from 94.2%, 97.5% and 82.7% to 92.0%, 96.3% and 76.4%, respectively. Such an operation is similar to PCB, which leverage 6 partial bins. The reason is that many persons are not well aligned in the images, and naively split the feature maps into a pre-defined number of bins cannot well resist to unaligned outliers. In addition, discriminative information may hardly be learned for some parts if we apply too dense division. In contrast, with our pyramid structure, we can formulate partial features from coarse to fine, which can finally form into a more robust feature representation for person images.

**Pooling Strategies** Row 4 and Row 5 in Table 6 shows the performance of HPM with different pooling strategies. It can be observed that max pooling performs better than average pooling in the most cases. The reason is that average pooling will take all locations of a particular parts into account and all the locations contribute equally to the final partial representation. Thus, the discriminative ability of the representation produced by average pooling can be easily influenced by the unrelated background patterns. In contrast, the global max pooling only preserve the largest response values for a local view. We consider these two pooling strategies are complementary in producing feature representations from global and local vies. Therefore, we integrate them into a unified model to take advantages from these two strategies. Experimental results in Table 6 demonstrate that mixing the two pooling strategies achieves better results compared with using either of them.

**Effectiveness of Horizontal Random Erasing** Table 7 shows the comparisons of HPM w/ and w/o applying horizontal random erasing for training. It can be observed that horizontal random erasing may not guarantee the best results in R1 or R5. However, it makes consistent im-

provements on the three benchmarks in mAP, which is the most important metrics to evaluate the effectiveness of Re-ID algorithms. The results proves that the horizontal random erasing can reduce the risk of over-fitting and improve the robustness of feature representation, especially on some small dataset (*e.g.* CUHK03).

## 5. Conclusion

In this work, we propose a novel Horizontal Pyramid Matching (HPM) approach to address the challenging person Re-ID task. The proposed HPM exploits partial information of each person to Re-ID, which successfully enhances the discriminative ability of partial feature and finally forms the into a more robust feature representation for the target person. In addition, we leverage both partial-based global average and max pooling to mine the discriminative information of each part in a global-local manner, which can further improve the robustness of partial features. We also introduce a simple yet effective random horizontal erasing operation to augment the model training. All the components detailed in this work can be easily embedded into any other framework to make a further performance improvement. Extensive ablation studies and comparisons well demonstrate the effectiveness of our HPM approach. In the future, we are planing to exploit more challenging Re-ID-related tasks, such as person Re-ID in the wild.

**Acknowledgements.** This work is in part supported by IBM-ILLINOIS Center for Cognitive Computing Systems Research (C3SR) - a research collaboration as part of the IBM AI Horizons Network. Shi is supported in part by IARPA Deep Intermodal Video Analytics (IARPA DIVA). Fu and Zhou are supported by CloudWalk Technology.

## References

- [1] E. Ahmed, M. Jones, and T. K. Marks. An improved deep learning architecture for person re-identification. In *Proceedings of the IEEE Conference on Computer Vision and Pattern Recognition*, pages 3908–3916, 2015.
- [2] X. Bai, M. Yang, T. Huang, Z. Dou, R. Yu, and Y. Xu. Deep-person: Learning discriminative deep features for person re-identification. *arXiv preprint arXiv:1711.10658*, 2017.
- [3] J. Bromley, I. Guyon, Y. LeCun, E. Säckinger, and R. Shah. Signature verification using a “siamese” time delay neural network. In *Advances in Neural Information Processing Systems*, pages 737–744, 1994.
- [4] X. Chang, T. M. Hospedales, and T. Xiang. Multi-level factorisation net for person re-identification. *arXiv preprint arXiv:1803.09132*, 2018.
- [5] W. Chen, X. Chen, J. Zhang, and K. Huang. A multi-task deep network for person re-identification. In *AAAI*, volume 1, page 3, 2017.
- [6] Y. Chen, X. Zhu, and S. Gong. Person re-identification by deep learning multi-scale representations. *2017 IEEE International Conference on Computer Vision Workshops (ICCVW)*, pages 2590–2600, 2017.
- [7] J. Deng, W. Dong, R. Socher, L.-J. Li, K. Li, and L. Fei-Fei. Imagenet: A large-scale hierarchical image database. In *Computer Vision and Pattern Recognition, 2009. CVPR 2009. IEEE Conference on*, pages 248–255. IEEE, 2009.
- [8] S. Ding, L. Lin, G. Wang, and H. Chao. Deep feature learning with relative distance comparison for person re-identification. *Pattern Recognition*, 48(10):2993–3003, 2015.
- [9] P. F. Felzenszwalb, R. B. Girshick, D. McAllester, and D. Ramanan. Object detection with discriminatively trained part-based models. *IEEE transactions on pattern analysis and machine intelligence*, 32(9):1627–1645, 2010.
- [10] I. Goodfellow, J. Pouget-Abadie, M. Mirza, B. Xu, D. Warde-Farley, S. Ozair, A. Courville, and Y. Bengio. Generative adversarial nets. In *Advances in neural information processing systems*, pages 2672–2680, 2014.
- [11] K. He, X. Zhang, S. Ren, and J. Sun. Spatial pyramid pooling in deep convolutional networks for visual recognition. In *European conference on computer vision*, pages 346–361. Springer, 2014.
- [12] K. He, X. Zhang, S. Ren, and J. Sun. Deep residual learning for image recognition. In *Proceedings of the IEEE conference on computer vision and pattern recognition*, pages 770–778, 2016.
- [13] A. Hermans, L. Beyer, and B. Leibe. In defense of the triplet loss for person re-identification. *arXiv preprint arXiv:1703.07737*, 2017.
- [14] R. Huang, S. Zhang, T. Li, R. He, et al. Beyond face rotation: Global and local perception gan for photorealistic and identity preserving frontal view synthesis. *arXiv preprint arXiv:1704.04086*, 2017.
- [15] C. Jose and F. Fleuret. Scalable metric learning via weighted approximate rank component analysis. In *European Conference on Computer Vision*, pages 875–890. Springer, 2016.
- [16] D. Li, X. Chen, Z. Zhang, and K. Huang. Learning deep context-aware features over body and latent parts for person re-identification. In *Proceedings of the IEEE Conference on Computer Vision and Pattern Recognition*, pages 384–393, 2017.
- [17] W. Li, R. Zhao, T. Xiao, and X. Wang. Deepreid: Deep filter pairing neural network for person re-identification. In *Proceedings of the IEEE Conference on Computer Vision and Pattern Recognition*, pages 152–159, 2014.
- [18] W. Li, X. Zhu, and S. Gong. Person re-identification by deep joint learning of multi-loss classification. In *IJCAI*, 2017.
- [19] W. Li, X. Zhu, and S. Gong. Harmonious attention network for person re-identification. *arXiv preprint arXiv:1802.08122*, 2018.
- [20] S. Liao, Y. Hu, X. Zhu, and S. Z. Li. Person re-identification by local maximal occurrence representation and metric learning. In *Proceedings of the IEEE Conference on Computer Vision and Pattern Recognition*, pages 2197–2206, 2015.
- [21] H. Liu, J. Feng, M. Qi, J. Jiang, and S. Yan. End-to-end comparative attention networks for person re-identification. *arXiv preprint arXiv:1606.04404*, 2016.
- [22] X. Liu, H. Zhao, M. Tian, L. Sheng, J. Shao, S. Yi, J. Yan, and X. Wang. Hydraplus-net: Attentive deep features for pedestrian analysis. *arXiv preprint arXiv:1709.09930*, 2017.
- [23] K. Simonyan and A. Zisserman. Very deep convolutional networks for large-scale image recognition. *arXiv preprint arXiv:1409.1556*, 2014.
- [24] K. K. Singh and Y. J. Lee. Hide-and-seek: Forcing a network to be meticulous for weakly-supervised object and action localization. In *The IEEE International Conference on Computer Vision*, 2017.
- [25] C. Su, J. Li, S. Zhang, J. Xing, W. Gao, and Q. Tian. Pose-driven deep convolutional model for person re-identification. In *2017 IEEE International Conference on Computer Vision (ICCV)*, pages 3980–3989. IEEE, 2017.
- [26] Y. Sun, L. Zheng, W. Deng, and S. Wang. Svdnet for pedestrian retrieval. *arXiv preprint*, 2017.
- [27] Y. Sun, L. Zheng, Y. Yang, Q. Tian, and S. Wang. Beyond part models: Person retrieval with refined part pooling. *arXiv preprint arXiv:1711.09349*, 2017.
- [28] C. Szegedy, V. Vanhoucke, S. Ioffe, J. Shlens, and Z. Wojna. Rethinking the inception architecture for computer vision. In *Proceedings of the IEEE Conference on Computer Vision and Pattern Recognition*, pages 2818–2826, 2016.
- [29] L. Wei, S. Zhang, W. Gao, and Q. Tian. Person transfer gan to bridge domain gap for person re-identification. *arXiv preprint arXiv:1711.08565*, 2017.
- [30] L. Wei, S. Zhang, H. Yao, W. Gao, and Q. Tian. Glad: Global-local-alignment descriptor for pedestrian retrieval. In *Proceedings of the 2017 ACM on Multimedia Conference*, pages 420–428. ACM, 2017.
- [31] Y. Wei, J. Feng, X. Liang, M.-M. Cheng, Y. Zhao, and S. Yan. Object region mining with adversarial erasing: A simple classification to semantic segmentation approach. In *IEEE CVPR*, 2017.

- [32] T. Xiao, H. Li, W. Ouyang, and X. Wang. Learning deep feature representations with domain guided dropout for person re-identification. In *Computer Vision and Pattern Recognition (CVPR), 2016 IEEE Conference on*, pages 1249–1258. IEEE, 2016.
- [33] T. Xiao, S. Li, B. Wang, L. Lin, and X. Wang. End-to-end deep learning for person search. *arXiv preprint*.
- [34] H. Yao, S. Zhang, Y. Zhang, J. Li, and Q. Tian. Deep representation learning with part loss for person re-identification. *arXiv preprint arXiv:1707.00798*, 2017.
- [35] D. Yi, Z. Lei, S. Liao, and S. Z. Li. Deep metric learning for person re-identification. In *Pattern Recognition (ICPR), 2014 22nd International Conference on*, pages 34–39. IEEE, 2014.
- [36] X. Zhang, H. Luo, X. Fan, W. Xiang, Y. Sun, Q. Xiao, W. Jiang, C. Zhang, and J. Sun. Alignedreid: Surpassing human-level performance in person re-identification. *arXiv preprint arXiv:1711.08184*, 2017.
- [37] H. Zhao, J. Shi, X. Qi, X. Wang, and J. Jia. Pyramid scene parsing network. In *IEEE Conf. on Computer Vision and Pattern Recognition (CVPR)*, pages 2881–2890, 2017.
- [38] L. Zhao, X. Li, Y. Zhuang, and J. Wang. Deeply-learned part-aligned representations for person re-identification. *2017 IEEE International Conference on Computer Vision (ICCV)*, pages 3239–3248, 2017.
- [39] L. Zheng, Z. Bie, Y. Sun, J. Wang, C. Su, S. Wang, and Q. Tian. Mars: A video benchmark for large-scale person re-identification. In *European Conference on Computer Vision*, pages 868–884. Springer, 2016.
- [40] L. Zheng, Y. Huang, H. Lu, and Y. Yang. Pose invariant embedding for deep person re-identification. *arXiv preprint arXiv:1701.07732*, 2017.
- [41] L. Zheng, L. Shen, L. Tian, S. Wang, J. Wang, and Q. Tian. Scalable person re-identification: A benchmark. In *Proceedings of the IEEE International Conference on Computer Vision*, pages 1116–1124, 2015.
- [42] L. Zheng, Y. Yang, and A. G. Hauptmann. Person re-identification: Past, present and future. *arXiv preprint arXiv:1610.02984*, 2016.
- [43] Z. Zheng, L. Zheng, and Y. Yang. A discriminatively learned cnn embedding for person reidentification. *ACM Transactions on Multimedia Computing, Communications, and Applications (TOMM)*, 14(1):13, 2017.
- [44] Z. Zheng, L. Zheng, and Y. Yang. Pedestrian alignment network for large-scale person re-identification. *arXiv preprint arXiv:1707.00408*, 2017.
- [45] Z. Zheng, L. Zheng, and Y. Yang. Unlabeled samples generated by gan improve the person re-identification baseline in vitro. *arXiv preprint arXiv:1701.07717*, 3, 2017.
- [46] Z. Zhong, L. Zheng, D. Cao, and S. Li. Re-ranking person re-identification with k-reciprocal encoding. In *Computer Vision and Pattern Recognition (CVPR), 2017 IEEE Conference on*, pages 3652–3661. IEEE, 2017.
- [47] Z. Zhong, L. Zheng, G. Kang, S. Li, and Y. Yang. Random erasing data augmentation. *arXiv preprint arXiv:1708.04896*, 2017.
- [48] Z. Zhong, L. Zheng, Z. Zheng, S. Li, and Y. Yang. Camera style adaptation for person re-identification. *arXiv preprint arXiv:1711.10295*, 2017.